Influence of projected climate change, urban expansion and heat adaptation strategies on end of 21st century urban boundary layer across the Conterminous US

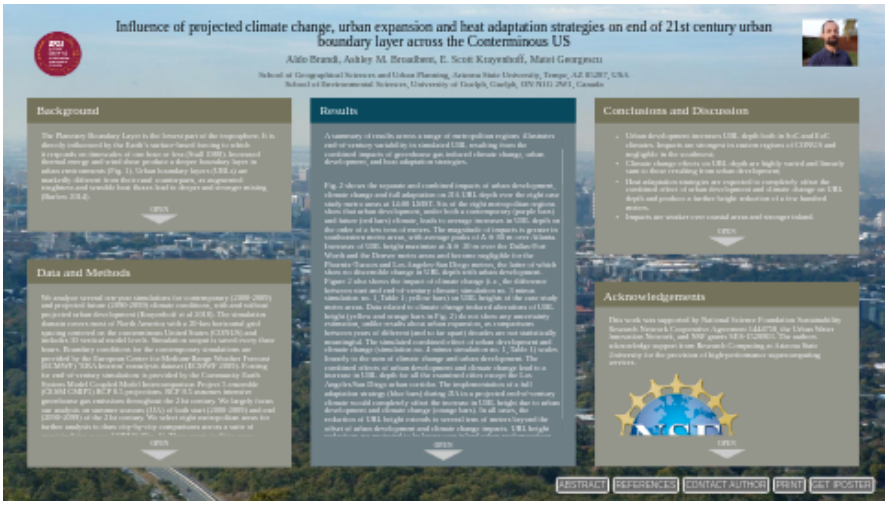

Aldo Brandi, Ashley M. Broadbent, E. Scott Krayenhoff, Matei Georgescu

School of Geographical Sciences and Urban Planning, Arizona State University, Tempe, AZ 85287, USA
School of Environmental Sciences, University of Guelph, Guelph, ON N1G 2W1, Canada

PRESENTED AT:

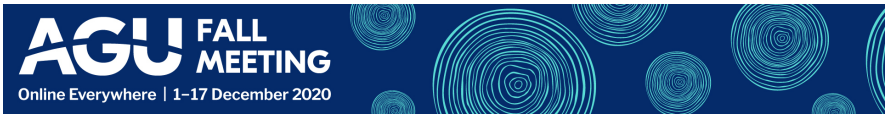

BACKGROUND

The Planetary Boundary Layer is the lowest part of the troposphere. It is directly influenced by the Earth's surface-based forcing to which it responds on timescales of one hour or less (Stull 1988). Increased thermal energy and wind shear produce a deeper boundary layer in urban environments (Fig. 1). Urban boundary layers (UBLs) are markedly different from their rural counterparts, as augmented roughness and sensible heat fluxes lead to deeper and stronger mixing (Barlow 2014).

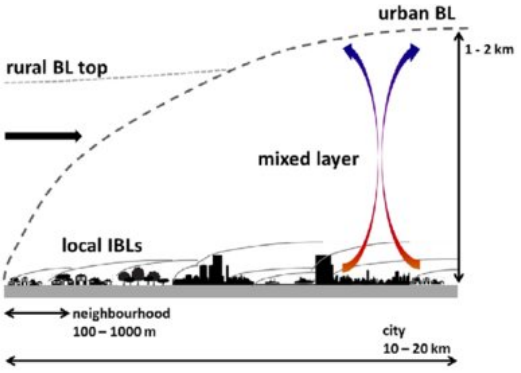

Schematic of Urban Boundary Layers. From Barlow, 2014.

Combined impacts of a warming climate and urban development (here defined as the combination of urban expansion and densification) are increasing the intensity and frequency of extreme heat events (Broadbent et al., 2020). As a consequence, heat adaptation has become a pressing priority for many cities, especially in the US and Europe. Commonly utilized thermal adaptation approaches achieve their objectives via modification of urban landscape properties.

Examples range from cool roofs and other reflective surfaces that reduce heat absorption of buildings and pavements by increasing surface albedo...

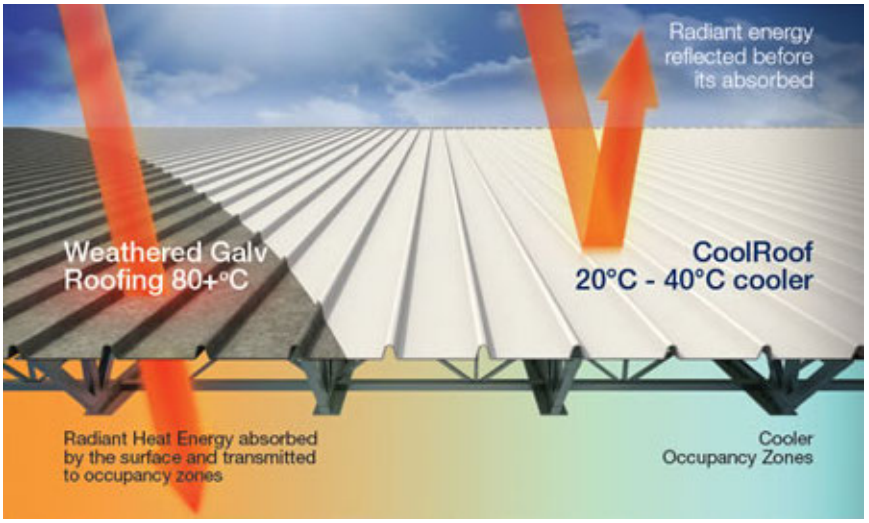

From https://www.spec-net.com.au

...to green and evaporative roofs that increase the latent fraction of turbulent heat flux partitioning through evapotranspiration processes of plants.

From http://nwrm.eu/measure/green-roofs (http://nwrm.eu/measure/green-roofs)

Some strategies, like street trees, provide shade over paved surfaces, reducing surface-absorbed solar energy while also permitting evapotranspiration.

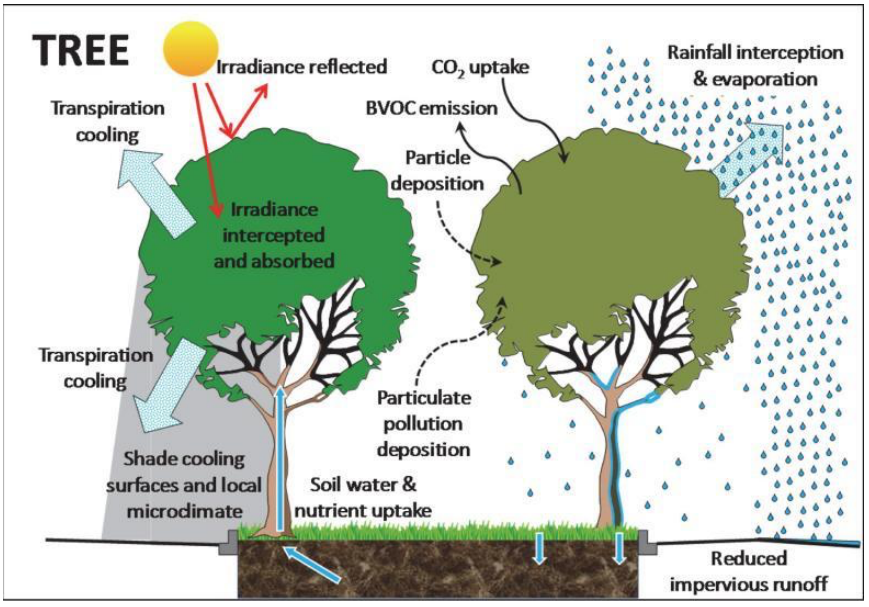

From Livesley et al. (2016)

Characterizing the evolution of UBLs is of particular importance since most human activities occur within this lowest portion of our atmosphere. Here we build on previous work to investigate the potential impacts associated with
explicit representation of end of 21 st century greenhouse gas induced climate change and urban development, including heat adaptation strategies, on UBLs across broad geographical scales (i.e. the Continental U.S.). We perform a detailed comparison of UBL dynamics across a range of climatic regions and cities. We consider several heat adaptation measures and assess their impacts on UBL both individually and simultaneously, and we pair such assessment to the analysis of changes in surface energy balance drivers. We use decadal scale WRF simulations of a suite of contemporary and projected futures across the continental US (CONUS) to investigate the combined impacts of greenhouse gas induced climate change, urban development, and heat adaptation strategies on UBL depth and structure. We provide a climatological assessment of the diurnal, seasonal and annual UBL impacts associated with heat adaptation in urban environments, focusing on a large geographical domain.

DATA AND METHODS

We analyze several ten-year simulations for contemporary (2000-2009) and projected future (2090-2099) climate conditions, with and without projected urban development (Krayenhoff et al 2018). The simulation domain covers most of North America with a 20-km horizontal grid spacing centered on the conterminous United States (CONUS) and includes 30 vertical model levels. Simulation output is saved every three hours. Boundary conditions for the contemporary simulations are provided by the European Center for Medium-Range Weather Forecast (ECMWF) 'ERA Interim' reanalysis dataset (ECMWF 2009). Forcing for end-of-century simulations is provided by the Community Earth System Model Coupled Model Intercomparison Project 5 ensemble (CESM CMIP5) RCP 8.5 projections. RCP 8.5 assumes intensive greenhouse gas emissions throughout the 21st century. We largely focus our analysis on summer seasons (JJA) of both start (2000-2009) and end (2090-2099) of the 21st century. We select eight metropolitan areas for further analysis to draw city-by-city comparisons across a suite of municipalities across CONUS (Fig. 1). These municipalities were chosen as they incorporate cities in different climatic regions and with varying urban development patterns.

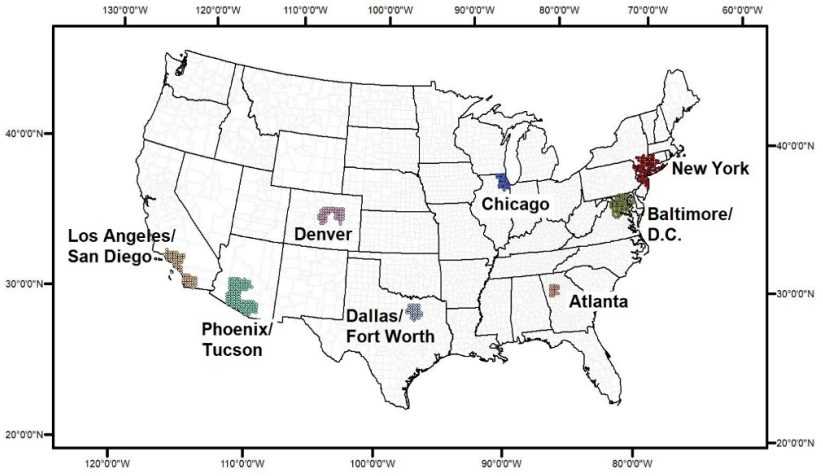

Fig. 1 *Geographical map of the Conterminous US, with state borders represented as black solid lines. Highlighted in colors are the urban regions/model cells considered for metropolitan-level analysis.*

WRF-ARW 3.6 Simulations

w/ Single Layer Urban Canopy Model

Spatial extent and resolution :

North America, 189 x 309 20km cells, 29 vertical levels

Temporal extent and resolution :

Start of Century (SoC) = 2000 - 2009

End of Century (EoC) = 2090 - 2099

8 simulation outputs per day

Climatological Forcing :

SoC = ECMWF 'ERA Interim' Reanalysis

EoC = CESM CMIP5 – RCP 8.5

Urban Extent:

EPA ICLUS 1.3.2 A2 SRES Scenarios (2010 and 2100)

We examine the climatological effect of a suite of heat adaptation scenarios, including cool roofs, green roofs and street trees. All roofing technologies are uniformly applied across CONUS city roofs to ascertain the maximum potential impact associated with the choice of strategy. For cool roofs, we incorporate a reflectivity of 0.88, the maximum Energy Star Solarflect value after 3 years of deterioration (Energy Star 2013). Green roofs are represented by evaporative roofs operating under the assumption of unlimited water availability. Street trees are parameterized to represent partial solar radiation penetration and account for diffuse radiation only (i.e., it is assumed there is no direct solar radiation beneath the tree canopy). In addition, to conserve energy, all intercepted shortwave radiation is converted into water vapor under the assumption of high soil water availability. Longwave radiation effects of trees, which are especially important for the simulation of the nighttime surface energy balance, are not accounted for here. Finally, a "Full Adaptation" scenario is implemented consisting of all three previously described strategies implemented simultaneously. Table 1 provides a list of all simulations used for the analysis. Additional information on climatological forcing, land

cover, urban development scenarios, model settings, and physics schemes utilized, including a comprehensive model evaluation across broad regions as well as across individual cities, can be found in Krayenhoff et al. (2018) and Broadbent et al (2020).

Full Adaptation Scenario

A combination of individual adaptation strategies

Cool Roofs :

.88 albedo, uniformly applied on all roofs across CONUS

Green Roofs :

Evaporating surfaces with unlimited water availability,

uniformly applied on all roofs across CONUS

Street Trees :

2.0 m2 m-2 Canyon Mean Leaf Area, distributed evenly

between heights 2.5 and 7.5 m in streets of all urban classes

Simulation Nº	Time period	GCM Forcing	Urban Land Cover	Adaptation Strategy
1	2000-2009	ECMWF	ICLUS A2 2010	No Adaptation
2	2000-2009	ECMWF	ICLUS A2 2100	No Adaptation
3	2090-2099	CESM (RCP 8.5)	ICLUS A2 2010	No Adaptation
4	2090-2099	CESM (RCP 8.5)	ICLUS A2 2100	No Adaptation
5	2090-2099	CESM (RCP 8.5)	ICLUS A2 2100	Cool roofs
6	2090-2099	CESM (RCP 8.5)	ICLUS A2 2100	Green roofs
7	2090-2099	CESM (RCP 8.5)	ICLUS A2 2100	Street trees
8	2090-2099	CESM (RCP 8.5)	ICLUS A2 2100	Full Adaptation (Cool roofs + Green roofs + Street trees)

Table 1 *Summary of all WRF simulations used in this study.*

RESULTS

A summary of results across a range of metropolitan regions illustrates end-of-century variability in simulated UBL resulting from the combined impacts of greenhouse gas induced climate change, urban development, and heat adaptation strategies.

Fig. 2 shows the separate and combined impacts of urban development, climate change and full adaptation on JJA UBL depth over the eight case study metro areas at 14:00 LMST. Six of the eight metropolitan regions show that urban development, under both a contemporary (purple bars) and future (red bars) climate, leads to average increases in UBL depth on the order of a few tens of meters. The magnitude of impacts is greater in southeastern metro areas, with average peaks of $\Delta \cong 80$ m over Atlanta. Increases of UBL height maximize at $\Delta \cong 20$ m over the Dallas-Fort Worth and the Denver metro areas and become negligible for the Phoenix-Tucson and Los Angeles-San Diego metros, the latter of which show no discernible change in UBL depth with urban development. Figure 2 also shows the impact of climate change (i.e., the difference between start and end-of-century climate; simulation no. 3 minus simulation no. 1, Table 1; yellow bars) on UBL heights of the case study metro areas. Data related to climate change induced alterations of UBL height (yellow and orange bars in Fig. 2) do not show any uncertainty estimation, unlike results about urban expansion, as comparisons between years of different (and so far apart) decades are not statistically meaningful. The simulated combined effect of urban development and climate change (simulation no. 4 minus simulation no. 1, Table 1) scales linearly to the sum of climate change and urban development. The combined effects of urban development and climate change lead to a increase in UBL depth for all the examined cities except the Los Angeles/San Diego urban corridor. The implementation of a full adaptation strategy (blue bars) during JJA in a projected end-of-century climate would completely offset the increase in UBL height due to urban development and climate change (orange bars). In all cases, the reduction of UBL height extends to several tens of meters beyond the offset of urban development and climate change impacts. UBL height reductions are projected to be larger over inland urban agglomerations (Atlanta, Chicago, Dallas-Fort Worth and Phoenix-Tucson) and smaller over coastal urban areas (New York, Baltimore-Washington D.C. and Los Angeles-San Diego).

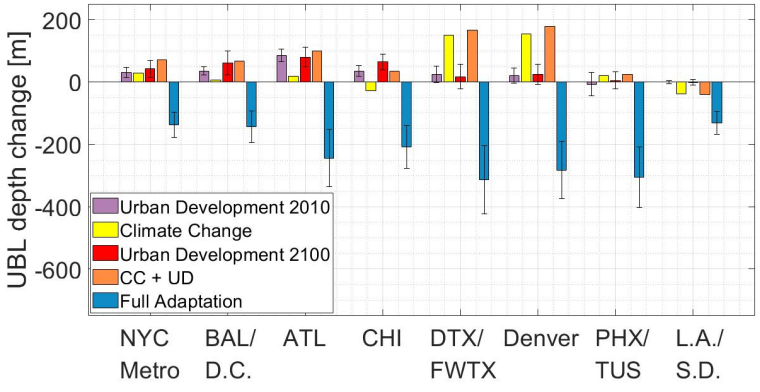

Fig. 2 *Summary of WRF simulated ten-year averaged summertime (JJA) showing physical drivers responsible for UBL impacts for eight US metropolitan areas undergoing urban expansion (ICLUS A2 2100) for a projected end of century climate (CESM RCP 8.5) at 14:00 LMST.*

It is instructive to ascertain the individual impacts of each heat adaptation measures on UBL height across the case study metropolitan regions examined. Fig. 3 shows a summary of impacts of all considered heat adaptation strategies on JJA UBL heights over the eight case study cities for a projected end-of-century climate at 14:00 LMST. The largest reduction in UBL depth is due to cool roofs, while green roofs have the smallest impact in all cities except Atlanta and Denver. The impacts of cool roofs, green roofs and full adaptation show greater reduction of UBL depth over inland urban regions, and smaller reduction over coastal urban regions. Street trees induced impacts show, instead, a more geographically uniform effect with a maximum UBL reduction ($\Delta \cong -100$ m) over Dallas-Fort Worth metro and a minimum ($\Delta \cong -40$ m) over Los Angeles-San Diego metro. The impacts from the three individual strategies do not sum linearly in the full adaptation scenario. The simulation of the simultaneous implementation of cool roofs, green roofs, and street trees produces impacts that are on average ~20% smaller than their linear sum, suggesting that impacts from individual strategies may mutually counterbalance.

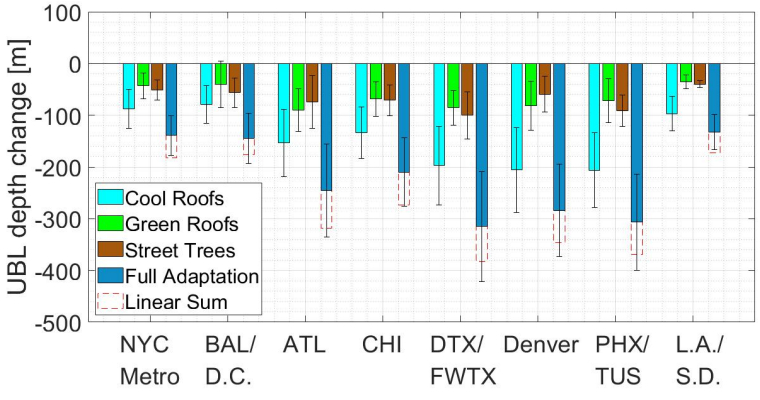

Fig. 3 *Summary of WRF simulated ten-year averaged summertime (JJA) UBL individual and combined heat adaptation impacts for eight US metropolitan areas undergoing urban expansion (ICLUS A2 2100) for a projected end of century climate (CESM RCP 8.5) at 14:00 LMST.*

We next examine annual composites of daily average values of UBL height, sensible and latent heat fluxes to explore seasonal trends in changes of the aforementioned variables over the eight case study metro areas. Fig. 4 shows that the reduction in UBL height is mostly driven by decreases in sensible heat flux (red bars). However, the magnitude of UBL depth reduction is not linearly related to the reduction in sensible heat flux. Full adaptation implementation is projected to increase ground heat flux everywhere across CONUS, and it is projected to increase latent heat flux in southwestern regions (Dallas/Fort Worth, Denver, Phoenix/Tucson, Los Angeles/San Diego). The magnitude of these increases is always smaller than the decreases in sensible heat flux, everywhere across CONUS.

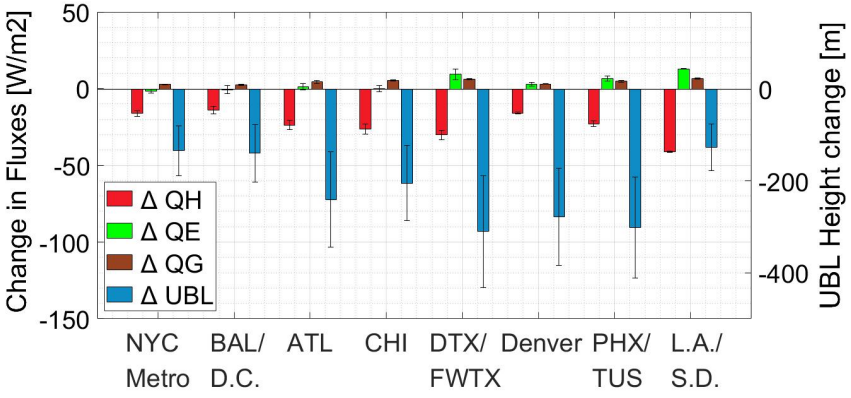

Fig. 4 *Summary of WRF simulated 10-year averaged summertime (JJA) full adaptation induced changes in surface energy balance components for eight US metropolitan areas undergoing urban expansion (ICLUS A2 2100) for a projected end of century climate (CESM RCP 8.5). Physical drivers responsible for full adaptation impacts on UBLs are: red bars – change in sensible heat flux (Δ QH); green bars – change in latent heat flux (Δ QE); brown bars – change in stored heat (Δ QG). Blue bars display the resulting impact of full adaptation on selected UBLs.*

Data from the Los Angeles/San Diego metro areas seem to present an anomaly. There, despite the largest reduction in sensible heat fluxes among the eight case study cities, the reduction in UBL height is the smallest in the sample. We then examine the annual evolution of heat fluxes for the Los Angeles/San Diego metro areas. Fig. 5 shows 10-year daily averaged changes in UBL height, sensible and latent heat fluxes due to full adaptation, over the metropolitan areas of Los Angeles and San Diego, in a projected end-of-century climate at 14:00 LMST. Despite the reduction in sensible heat flux (purple dashed line in Fig. 5b), illustrating a clear seasonal trend with a maximum reduction (Δ ≅ -180 W/m2) in mid-July, UBL depth reduction stays constant at Δ ≅ -100 m throughout the year (blue dashed line in Fig. 5a). This discrepancy may be explained by a concurrent summer increase in latent heat flux (Δ ≅ 50 W/m2, green dashed line in Fig. 5b), which may add thermal energy to the atmosphere thus reducing its static stability.

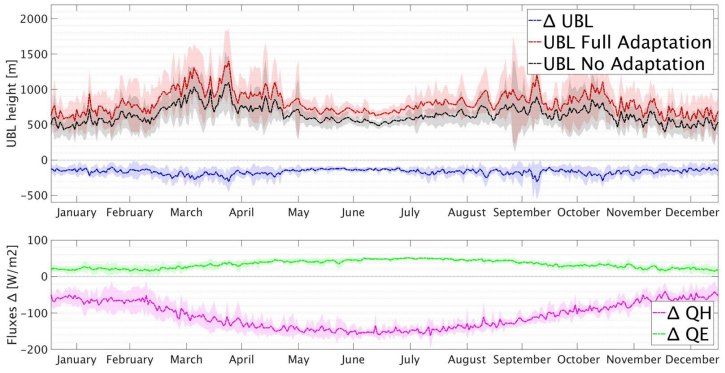

Fig 5 *Annual average composite of* ***a*** *UBL depth over the Los Angeles and San Diego metropolitan areas undergoing urban expansion (ICLUS A2 2100) for a projected end of century climate (CESM RCP 8.5).* ***b*** *represents the differences (Full Adaptation minus No Adaptation in sensible (QH) and latent (QE) heat fluxes due to Full Adaptation implementation. Shades represent 1σ standard deviation about the 10-year average. Time shown is 14:00 LMST.*

The impact of latent heat flux increase due to heat adaptation strategies is also evident in Fig. 6. Here, 10-year averages of 14:00 (LMST) JJA potential temperature differences between no adaptation (simulation no. 4, Table 1) and heat adaptation strategies (simulations no. 5-8, Table 1) are presented for the NYC metro-region (Fig. 6a) and Los Angeles and San Diego (Fig. 6b) metro areas. The magnitude of potential temperature reduction at the lowest model level due to full adaptation strategies is smaller in New York (Δ ≅ -0.9 K, Fig. 9a) than in the Los Angeles and San Diego metro areas (Δ ≅ -1.43 K, Fig. 6b). However, the vertical extent of potential temperature

reduction is more than 700 m higher over the New York metro-area (red line marker in Fig. 6a.) than across the Los Angeles/San Diego corridor (red line marker in Fig. 6b), possibly as a consequence of increased latent heat fluxes.

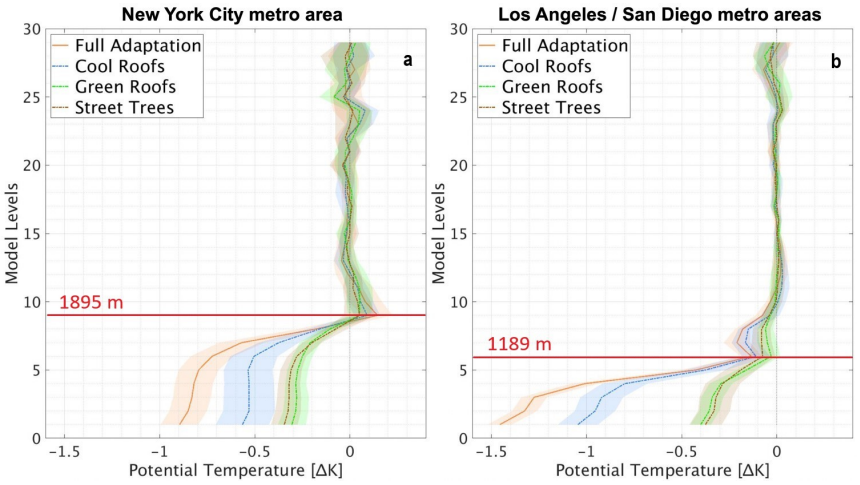

Fig. 6 *Ten-year averages of summertime (JJA) potential temperature differences between no adaptation and adaptation scenarios for a New York and b Los Angeles and San Diego metropolitan areas undergoing urban expansion (ICLUS A2 2100) for a projected end of century climate (CESM RCP 8.5) at 14:00 LMST. Shaded areas represent 1σ standard deviation of averages.*

The decreasing impact of full adaptation strategies on potential temperature lapse rates persist throughout the nighttime, reinforcing the static stability of the nocturnal boundary layer for all eight case study metro areas affected by urban development (ICLUS 2100) for a projected end-of-century summertime climate (CESM 2100). Increases in static stability are greater for cities characterized by more humid background climates, with peak nocturnal reduction over the Dallas/Fort Worth metro areas (Δ ≅ -1.1 K, Fig. 7), and reduced impacts over more arid metro areas with minimum impact over the Los Angeles and San Diego metro areas (Δ ≅ -0.2 K, Fig. 7).

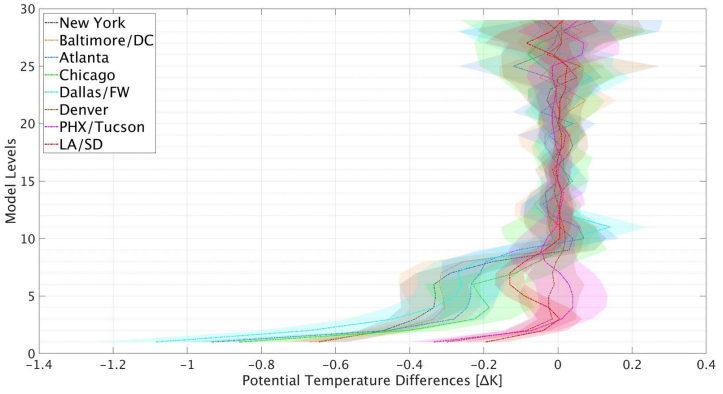

Fig. 7 *Ten-year averages of summertime (JJA) potential temperature differences between no adaptation and full adaptation scenarios (Full Adaptation minus No Adaptation) for all case study metropolitan areas undergoing urban expansion (ICLUS A2 2100) for a projected end of century climate (CESM RCP 8.5). The time shown is 02:00 LMST. Shaded areas represent 1σ standard deviation of the 10-year averages. Full adaptation includes cool roofs, green roofs and street trees simultaneously implemented.*

The impact of heat adaptation strategies on UBL depth and potential temperature lapse rates extends to regional-scale dynamics and vertical wind profiles. The implementation of heat adaptation strategies reduces the magnitude of vertical winds, with peak reductions due to full adaptation ranging from Δ ≅ -.006 m/s in the New York metro-region to Δ ≅ -.045 m/s over the Phoenix-Tucson metro areas. Consistent with the impact on all other meteorological parameters analyzed, the greatest impact on vertical winds arises from cool roof deployment. In all case study cities, except Denver, heat adaptation strategies promote earlier and stronger subsidence in the upper UBL. In the arid regions of the south and southwest this reversal effect becomes considerably intense, reaching downward speeds of $w < -.05$ m/s at the top of the summertime boundary layer (h ≅ 3000 m) over the Phoenix and Tucson metro areas (Fig. 8). Fig. 8 shows the same pattern of impacts as was previously presented in Figs. 6 and 9. The most effective individual heat adaptation strategy in reducing vertical winds are cool roofs, and the impact due to full adaptation is smaller than the linear sum of individual impacts (~40% smaller over Phoenix and Tucson metro areas).

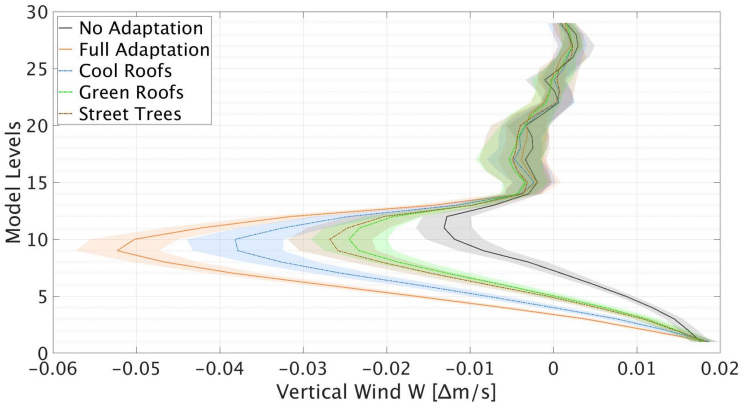

Fig. 8 *Ten-year averages of seasonal vertical wind speed changes due to Full Adaptation implementation over the Phoenix and Tucson metropolitan areas undergoing urban expansion for a projected end of century climate (CESM RCP 8.5). Black line represents vertical wind profiles in a No-Adaptation scenario. Orange line represents vertical wind profiles in a Full Adaptation scenario. Dashed lines represent vertical wind profiles for each individual adaptation strategy: blue line represents the impact of cool roofs implementation; green line represents the impact of green roofs implementation; brown line represents the impact of street trees implementation. Shaded areas represent 1σ standard deviation of the 10-year averages. The time shown is 14:00 LMST. Full adaptation includes cool roofs, green roofs and street trees simultaneously implemented.*

CONCLUSIONS AND DISCUSSION

- Urban development increases UBL depth both in SoC and EoC climates. Impacts are strongest in eastern regions of CONUS and negligible in the southwest;
- Climate change effects on UBL depth are highly varied and linearly sum to those resulting from urban development;
- Heat adaptation strategies are expected to completely offset the combined effect of urban development and climate change on UBL depth and produce a further height reduction of a few hundred meters.
- Impacts are weaker over coastal areas and stronger inland.
- Largest reductions in UBL depth are due to Cool roofs, which are mostly responsible for the reduction in sensible heat fluxes;
- Green roofs have the smallest impact in all cities except Atlanta and Denver;
- Street trees induced impacts are more geographically uniform;
- The impacts from the three individual strategies do not sum linearly in the full adaptation scenario (20% smaller).
- Increased latent heat flux (QE) adds moisture and thermal energy to the lower atmosphere, reducing static stability;
- Increases in latent heat fluxes may dampen UBL depth reduction by counterbalancing sensible heat flux (QH) reduction
- Heat adaptation strategies increase (daytime and nighttime) static stability and reduce vertical winds promoting subsidence.

The reduction of UBL depth and convective mixing may have important consequences on air quality, as it reduces the volume of air available for pollutants dilution and dispersion. That is especially true near the surface where most human activities take place. The reduction of vertical transport of moisture can also be detrimental in cloud formation processes, and consequently reduce the amount of precipitation in urban or their downwind environments. Our results highlight the importance of considering the tradeoffs associated with the implementation of heat adaptation strategies. This study helps inform the discussion surrounding the diverse impacts associated with heat adaptation in urban environments and supports continued efforts focused on development of increasingly resilient future cities that preserve the health of their dwellers.

An extended version of this analysis is under review for pubblication (Brandi et al. 2021).

ACKNOWLEDGEMENTS

This work was supported by National Science Foundation Sustainability Research Network Cooperative Agreement 1444758, the Urban Water Innovation Network, and NSF grants SES-1520803. The authors acknowledge support from Research Computing at Arizona State University for the provision of high-performance supercomputing services.

ABSTRACT

The urban environment directly influences the evolution of the Urban Boundary Layer (UBL). Heat adaptation strategies proposed to help cities respond to global change and urban induced warming, are also expected to reduce the intensity of convective mixing and decrease UBL depth, thereby reducing the volume of air available to pollutant dilution and dispersion. We use 20 km resolution WRF-ARW decadal scale simulations that account for end of 21st century greenhouse gas emissions, urban expansion and intensive and uniform implementation of cool roofs, green roofs and street trees to investigate the individual and combined impacts of these drivers on the dynamics of the UBL over the Conterminous US (CONUS). Results indicate that combined impacts of climate change and urban expansion are expected to increase summer (JJA) daytime UBL depth in the eastern regions of CONUS (peak value: $\Delta h \cong 80$ m over Atlanta metro area). When adaptation strategies are applied, summer daytime UBL depth is reduced by a few hundred meters (peak value: $\Delta h \cong -310$ m over Dallas and Fort Worth metro areas) in all CONUS regions as a consequence of decreased surface sensible heat fluxes. Adaptation impacts are greater inland and smaller over coastal cities. In arid regions, the adaptation induced increase in latent heat fluxes can counterbalance the projected decrease in UBL depth. Furthermore, adaptation strategies are expected to increase the static stability of both daytime and nighttime UBLs and decrease the magnitude of vertical winds, inducing earlier and stronger subsidence (peak value: $\Delta m/s \cong -0.05$ m over Phoenix and Tucson metro areas). In light of these findings, ongoing work addressing these aspects with convection resolving, high-resolution simulations is needed to determine whether the widespread implementation of urban adaptation measures could have deleterious effects for urban air quality in the cities of the future Contiguous US.

REFERENCES

Barlow, J. F. (2014). Progress in observing and modelling the urban boundary layer. Urban Climate, 10, 216-240.

Broadbent, A. M., Krayenhoff, E. S., & Georgescu, M. (2020). The motley drivers of heat and cold exposure in 21st century US cities. Proceedings of the National Academy of Sciences, 117(35), 21108-21117.

Brandi, A., Broadbent, A. M., Krayenhoff, E. S., & Georgescu, M. (2021) Influence of projected climate change, urban expansion and heat adaptation strategies on end of 21st century urban boundary layer across the Conterminous US. Climate Dynamics. "In Review"

ENERGY STAR Roof Product List (Energy Star, 2013); https://go.nature.com/2CuhGPn

Krayenhoff, E. S., Moustaoui, M., Broadbent, A. M., Gupta, V., & Georgescu, M. (2018). Diurnal interaction between urban expansion, climate change and adaptation in US cities. Nature Climate Change, 8(12), 1097-1103

Livesley, S. J., McPherson, E. G., & Calfapietra, C. (2016). The urban forest and ecosystem services: impacts on urban water, heat, and pollution cycles at the tree, street, and city scale. Journal of environmental quality, 45(1), 119-124.

Stull, R. B. (2012). An introduction to boundary layer meteorology (Vol. 13). Springer Science & Business Media.